Method II

Broer, H.; Hoveijn, I.; Lunter, G.; Vegter, G.

Published in:
EPRINTS-BOOK-TITLE

Publication date:
2003

3 Method II: The energy-momentum map

In this chapter we apply the energy–momentum map reduction method to the same class of systems as in Chap. 2, namely two degree-of-freedom systems with optional symmetry, near equilibrium and close to resonance. We calculate the tangent space and nondegeneracy conditions for the 1:2, 1:3 and 1:4 resonances starting from a Birkhoff normalized Hamiltonian. The case of the spring-pendulum close to 1:2 resonance is treated in more detail. We arrive at a polynomial model which is different from the one found in Chap. 2, and which has an additional saddle–node bifurcation.

3.1 Introduction

Several methods for analyzing Hamiltonian systems around resonance are available. One is the planar reduction method [BCKV95, BCKV93] of the previous chapter, but many more are available, see e.g. [Arn93a, GMSD95, SV85, Sch74] and references there. This chapter uses a method introduced in [Dui84, Sch74]. Just as the planar reduction method of Chap. 2, it uses the Birkhoff procedure followed by symmetric reduction. The singularity theory used subsequently is different, however, and uses left-right transformations to normalize a certain map from phase space to $\mathbb{R}^2$, the *energy–momentum map*. The remainder of the approach is again similar to that of Chap. 2: From a normal form of the map we compute bifurcation curves, and by explicitly computing the singularity theory transformations these are pulled back to original coordinates and parameters.

The algorithms we use to compute the reparametrizations (and the bifurcation curves) are closely related to those used in the previous chapter. Both Kas and Schlessinger's algorithm and the division algorithm have their counterparts in the present setting. With the planar reduction method of the previous chapter, the tangent space is an ideal, leading to a division algorithm that could be borrowed from Gröbner basis theory with little modification. The energy–momentum map method leads to a more complicated tangent space. These complications surface again in the division algorithm. In fact the complications were such that modifying the previous approach in an *ad-hoc* manner turned out to be infeasible. Instead we used a structured approach that brought, amongst others, Gröbner bases and standard bases for both tangent spaces into a common framework. Within this framework it was possible to derive the required division

H. Broer, I. Hoveijn, G. Lunter, and G. Vegter: LNM 1806, pp. 45–68, 2003.

algorithm systematically. These results are described in Chaps. 6 and 7, and are applied in this chapter.

We now give an overview of the energy–momentum map method. For a general outline of this (and other) reduction methods, see the introduction to Chap. 2; here we shall be brief. After the Birkhoff procedure and truncation (or, modulo a flat perturbation), the system acquires an $\mathbb{S}^1$ symmetry, with associated conserved quantity H_2. We then construct the energy–momentum map $\boldsymbol{E}$, mapping phase space to $\mathbb{R}^2$. Its first component is the Hamiltonian, and the second component is the conserved quantity H_2. This map encodes information about the dynamics of Birkhoff-normalized system: Its fibers are invariant manifolds of the system, with singular points corresponding to periodic orbits. Both the fibers and singular points of $\boldsymbol{E}$ are smoothly deformed under the group of near-identity left-right transformations (B, A), with group operation $(B', A') * (B, A) = (B' \circ B, A \circ A')$, and action

$$\boldsymbol{E} \mapsto B \circ \boldsymbol{E} \circ A.$$

Since after the Birkhoff procedure the system has a (formal) circle symmetry, the map $\boldsymbol{E}$ has this symmetry too. It is necessary to do the singularity theory inside the space of symmetric mappings, since the orbit of $\boldsymbol{E}$ under left-right transformations has infinite codimension in the general space. Hence, we must also restrict to right-transformations A that commute with the symmetry. Instead of doing this explicitly, we reduce the symmetry by using circle-symmetric coordinates. For a 2 degree-of-freedom system, we thus can reduce from a circle-invariant map on $\mathbb{R}^4$, to a map on $\mathbb{R}^3$ that respects a certain algebraic relation between the variables.

Just as in the planar reduction method, dynamical conjugacy is lost with arbitrary (circle-equivariant but non-symplectic) right-transformations. However, if the system has 2 degrees of freedom, it lives on a 4-dimensional phase space, and nondegenerate fibers of $\boldsymbol{E}$ are 2-dimensional circle-invariant manifolds. After symmetry reduction we get 1-dimensional dynamically invariant manifolds, i.e., orbits of the reduced system. A universal deformation of $\boldsymbol{E}$ (i.e., a transversal section to its orbit under left-right transformations) can be related to a such a system that is *equivalent*, i.e., conjugate modulo a time-reparametrization, to the reduced Birkhoff-normalized system, again, just as in the planar reduction method.

In contrast to that method, it is not easy to de-reduce to the full system after normalization, because the fibers $H_2 =$ constant are not preserved by the normalizing transformations (even though, after [Dui84], the transformations we use preserve $\boldsymbol{E}$'s second component). The present method therefore seems less suited for studying the flat perturbations; see [BCKV95, BCKV93] for more remarks. Our current goal remains to pull back bifurcation curves. Although the larger class of allowed transformations necessitates an extra calculation to obtain the H_2-level at the bifurcation point, this turns out to be straightforward in this case.

A summary of this chapter was published as [Lun99b].

3.2 Description of the method

This section describes the general energy–momentum map method in detail. It follows [Dui84] to great extent. To avoid cluttering the formulas, the system's dependence on parameters and coefficients is suppressed in this section. From Sect. 3.4 onwards this dependence will be explicitly taken into account again.

3.2.1 Birkhoff normalization

The first step is Birkhoff normalization. Assume the Hamiltonian H has vanishing linear part. Then, after truncation (or modulo a flat perturbation) the Birkhoff-normalized Hamiltonian H^n is $\mathbb{S}^1$-symmetric, and assumes the form

$$H^n = H_2^0 + f_0(\rho_1, \rho_2, \psi, \chi), \tag{3.1}$$

where we expressed the normalized Hamiltonian in the invariants

$$\rho_1 = z_1\bar{z}_1, \quad \rho_2 = z_2\bar{z}_2, \quad \psi = \frac{1}{2}(z_1^p\bar{z}_2^{|q|} + \bar{z}_1^p z_2^{|q|}), \quad \chi = \frac{1}{2\mathrm{i}}(z_1^p\bar{z}_2^{|q|} - \bar{z}_1^p z_2^{|q|}),$$

and $H_2^0 = \mathrm{i}\rho_1 + \mathrm{i}\omega\rho_2$, with $\omega = \frac{p}{q}$, is an integral of motion. Note that H^n, and thus also f_0, depend on several parameters. In the case of the $1:2$ and $1:-2$ resonances, a second symplectic normalization removes the dependence on χ. This is a consequence of the unique normal form for Hamiltonians for these resonances; see [SvdM92].

Proposition 3.1. *Suppose $p:q = 1:\pm 2$ and the coefficients of ψ and χ in H^n do not both vanish. Then there exists a symplectic coordinate transformation that brings the Hamiltonian (3.1) in the form*

$$H^N = H_2^0 + f_1(\rho_1, \rho_2, \psi). \tag{3.2}$$

For a proof, see Sect. 4.3.2. In [Dui84] the dependence on χ is removed by a non-symplectic transformation. The present method leads to a shorter calculation, since we can calculate with Hamiltonians instead of vector fields. A preliminary calculation suggested that this approach cannot be used for higher resonances.

Remark 3.2. *(Comparison with Proposition 2.2)* Note that we arrived at (3.2) without assuming a time-reversal symmetry on H. This may be contrasted to the result of Proposition 2.2, where this assumption was needed. However, the current result only holds for the $1:2$ resonance, whereas Proposition 2.2 is more general.

3.2.2 Circle-equivariant vector fields

In this section we calculate generators for the module of vector fields equivariant under the H_2^0-circle action, under which the system is invariant after Birkhoff normalization. We pick the main line of the argument up again in Sect. 3.2.3.

From now on, we work in the ring of formal power series in the fundamental invariants, $R = \mathbb{R}[[\rho_1, \rho_2, \psi, \chi]]$, instead of $\mathbb{R}[[z_1, \bar{z}_1, z_2, \bar{z}_2]]$. There is one relation between the variables, namely

$$\psi^2 + \chi^2 - \rho_1^p \rho_2^q = 0. \tag{3.3}$$

For the $1 : \pm 2$ resonance cases, we can restrict to $\mathbb{R}[[\rho_1, \rho_2, \psi]]$ right away, and use the relation $\psi^2 - \rho_1^p \rho_2^q = 0$. We first deal with the general case.

Arbitrary resonances A circle-equivariant vector field in the variables $z_1, \bar{z}_1$, $z_2, \bar{z}_2$ corresponds to a vector field in $\rho_1, \rho_2, \psi, \chi$-space that leaves the relation (3.3) invariant. Such a vector field can always be written as

$$\boldsymbol{\alpha} = f_1 \frac{\partial}{\partial \rho_1} + f_2 \frac{\partial}{\partial \rho_2} + f_3 \frac{\partial}{\partial \psi} + f_4 \frac{\partial}{\partial \chi}.$$

The derivative of $\psi^2 + \chi^2 - \rho_1^p \rho_2^q$ in the direction of $\boldsymbol{\alpha}$ is

$$-p f_1 \rho_1^{p-1} \rho_2^q \; - \; q f_2 \rho_1^p \rho_2^{q-1} \; + \; 2 f_3 \psi \; + \; 2 f_4 \chi.$$

Requiring this to be an element of $\left\langle \psi^2 + \chi^2 - \rho_1^p \rho_2^q \right\rangle_R$ leads to conditions on the f_i and the exponents p, q, in turn leading to the following generators $\mathbf{v}_i$ of the R-module of equivariant vector fields:

	f_1	f_2	f_3	f_4
$\mathbf{v}_1$	$2\rho_1$		$p\psi$	$p\chi$
$\mathbf{v}_2$		$2\rho_2$	$q\psi$	$q\chi$
$\mathbf{v}_3$			χ	$-\psi$
$\mathbf{v}_4$	2ψ		$p\rho_1^{p-1}\rho_2^q$	
$\mathbf{v}_5$	2χ			$p\rho_1^{p-1}\rho_2^q$
$\mathbf{v}_6$		2ψ	$q\rho_1^p\rho_2^{q-1}$	
$\mathbf{v}_7$		2χ		$q\rho_1^p\rho_2^{q-1}$

These generators are independent over R, in the sense that there is no relation $\mathbf{v}_i = \sum_{j \neq i} f_j \mathbf{v}_j$ with $f_j \in R$, for any i. Below we shall need the derivative of H_2 along an arbitrary circle-invariant vector field $\boldsymbol{\alpha}$. So let $\boldsymbol{\alpha}$ be

$$\boldsymbol{\alpha} = v_1 \mathbf{v}_1 + \cdots + v_7 \mathbf{v}_7,$$

where $v_i \in R$, then the derivative of H_2 with respect to $\boldsymbol{\alpha}$ is

$$\boldsymbol{\alpha} H_2 \; = \; \boldsymbol{\alpha}(q\rho_1 + p\rho_2) \; = \; 2qv_1\rho_1 + 2pv_2\rho_2 + 2(qv_4 + pv_6)\psi + 2(qv_5 + pv_7)\chi. \tag{3.4}$$

Note that we wrote, for convenience, $H_2 = q\rho_1 + p\rho_2$, which differs from the quadratic part of H^N in (3.2) by a factor i/q; since we are interested in the location of critical points, this difference is immaterial.

The resonances 1 : ±2 An arbitrary vector field now takes the form $\boldsymbol{\alpha} = f_1\frac{\partial}{\partial\rho_1} + f_2\frac{\partial}{\partial\rho_2} + f_3\frac{\partial}{\partial\psi}$, and the condition that the derivative of the relation $\psi^2 - \rho_1^p\rho_2^q$ along $\boldsymbol{\alpha}$, which is $-pf_1\rho_1^{p-1}\rho_2^q - qf_2\rho_1^p\rho_2^{q-1} + 2f_3\psi$, is an element of the ideal generated by the relation, yields the following generators of the module of equivariant vector fields:

	f_1	f_2	f_3
$\mathbf{v}_1$	$2\rho_1$		$p\psi$
$\mathbf{v}_2$		$2\rho_2$	$q\psi$
$\mathbf{v}_4$	2ψ		$p\rho_1^{p-1}\rho_2^q$
$\mathbf{v}_6$		2ψ	$q\rho_1^p\rho_2^{q-1}$

The numbering of the generators is chosen to stress the relation with the previous case. An arbitrary circle-equivariant vector field, and the derivative of H_2 along it, now take the form

$$\begin{aligned} \boldsymbol{\alpha} &= v_1\mathbf{v}_1 + v_2\mathbf{v}_2 + v_4\mathbf{v}_4 + v_6\mathbf{v}_6, \\ \boldsymbol{\alpha}H_2 &= 2qv_1\rho_1 + 2pv_2\rho_2 + 2(qv_4 + pv_6)\psi. \end{aligned} \tag{3.5}$$

3.2.3 The energy–momentum map

We now introduce the main object of interest, the energy–momentum map:

$$\boldsymbol{E}: \quad \mathbb{R}^4 \to \mathbb{R}^2: \quad (\rho_1, \rho_2, \psi, \chi) \mapsto (H^n, H_2^0).$$

Here H^n is the Hamiltonian in Birkhoff normal form, depending on the parameters, and H_2^0 is the quadratic part of H^n when the parameters vanish (see also Chap. 4, remark 4.5). Note that the relation $\psi^2 + \chi^2 - \rho_1^p\rho_2^q = 0$ is supposed to hold, so that it suffices to define $\boldsymbol{E}$ on the variety of points satisfying the relation, but we do not make this explicit in the notation.

The fibers of $\boldsymbol{E}$ are invariant under the flow of H^n. They are smoothly deformed by left-right transformations (A, B), where $A : \mathbb{R}^4 \to \mathbb{R}^4$ are circle-equivariant near-identity diffeomorphisms on $\mathbb{R}^4$, and $B : \mathbb{R}^2 \to \mathbb{R}^2$ are arbitrary planar near-identity diffeomorphisms, with action

$$(A, B): \quad \boldsymbol{E} \mapsto B \circ \boldsymbol{E} \circ A.$$

In the context of unfoldings, the left-right transformation (A, B) depends on parameters, and is the identity mapping at the origin in parameter space. The set of invertible left-right transformations forms a group, with the obvious composition as group operation. To find a universal deformation of $\boldsymbol{E}$, we look at the tangent space, at $\boldsymbol{E}$, to the orbit of $\boldsymbol{E}$ under the action of the group. This tangent space is

$$T_{\boldsymbol{E}} = \{(\boldsymbol{\alpha}H + \beta_1(H, H_2), \boldsymbol{\alpha}H_2 + \beta_2(H, H_2))\},$$

where $\boldsymbol{\alpha}$ runs over the circle-equivariant vector fields, and β_i are arbitrary functions of 2 variables, see Sect. 5.4.

The set $T_{\boldsymbol{E}}$ is a subset of $R \oplus R$, the space of maps from $\mathbb{R}^n$ to $\mathbb{R}^2$ (recall that $R = \mathbb{R}[[\rho_1, \rho_2, \psi, \chi]]$). It is possible to reduce $T_{\boldsymbol{E}}$ to a subset of R in the following way. Consider the map T going from the tangent space of the group of left-right transformations at the identity element, to $R \oplus R$, defined by

$$T: \quad (\boldsymbol{\alpha}, \beta_1, \beta_2) \mapsto (\boldsymbol{\alpha}H + \beta_1(H, H_2), \boldsymbol{\alpha}H_2 + \beta_2(H, H_2)).$$

We have $\operatorname{Im} T = T_{\boldsymbol{E}}$. From (3.4) it follows that the image of the second component of T, denoted by T_2, maps surjectively into R. Therefore, since T is a linear map, the codimension of $T_{\boldsymbol{E}}$ in $R \oplus R$ is the codimension in R of the image of T_1, restricted to the kernel of T_2. In other words, to compute the codimension of $T_{\boldsymbol{E}}$, we may restrict to left-right transformations that do not alter the second component of $\boldsymbol{E}$, and look at how those transformations change its first component. If the codimension of $T_1(\ker T_2) \subseteq R$ is finite, and $t_1, \ldots, t_d$ are complementing elements, then the elements $(t_1, 0), \ldots, (t_d, 0)$ span a complement of $T_{\boldsymbol{E}}$. By the results of Chap. 5, this immediately gives a universal deformation of $\boldsymbol{E}$, say F, namely $F : \mathbb{R}^4 \oplus \mathbb{R}^d \to \mathbb{R}^2 : (x, u) \mapsto \boldsymbol{E} + u_1 \cdot (t_1, 0) + \cdots + u_d \cdot (t_d, 0)$ We shall denote the space $T_1(\ker T_2)$ by $T^r_{\boldsymbol{E}}$, the *reduced* tangent space to $\boldsymbol{E}$. This reduced tangent space takes the following form:

$$T^r_{\boldsymbol{E}} := \{\boldsymbol{\alpha}H + \beta_1(H, H_2) | \boldsymbol{\alpha}H_2 + \beta_2(H, H_2) = 0\}, \tag{3.6}$$

where $\boldsymbol{\alpha}$ runs over the circle invariant vector fields, and β_i over the arbitrary functions in two variables. From (3.4) it follows that $\boldsymbol{\alpha}H_2$ vanishes at the origin, hence β_2 can be written as $\beta_2(x, y) = x\gamma_1(x, y) + y\gamma_2(x, y)$. Also from (3.4) it follows that for every function f vanishing at the origin, there exists a vector fields $\boldsymbol{\alpha}$ with $\boldsymbol{\alpha}H_2 = f$. In particular, let $\boldsymbol{\alpha}_1$ and $\boldsymbol{\alpha}_2$ be defined by

$$\begin{aligned} \boldsymbol{\alpha}_1 H_2 &= H, \\ \boldsymbol{\alpha}_2 H_2 &= H_2. \end{aligned}$$

Then, writing $\beta_2(H, H_2) = H\gamma_1(H, H_2) + H_2\gamma_2(H, H_2)$, the reduced tangent space can be written as

$$T^r_{\boldsymbol{E}} = \{\boldsymbol{\alpha}H + \beta_1(H, H_2) | \left(\boldsymbol{\alpha} + \gamma_1(H, H_2)\boldsymbol{\alpha}_1 + \gamma_2(H, H_2)\boldsymbol{\alpha}_2\right) H_2 = 0\},$$

and with a change of variables $\boldsymbol{\alpha}' = \boldsymbol{\alpha} + \gamma_1\boldsymbol{\alpha}_1 + \gamma_2\boldsymbol{\alpha}_2$ it becomes

$$T^r_{\boldsymbol{E}} = \{\boldsymbol{\alpha}'H + f_1\gamma_1(H, H_2) + f_2\gamma_2(H, H_2) + \beta_1(H, H_2) | \boldsymbol{\alpha}'H_2 = 0\},$$

where we wrote

$$f_i = -\boldsymbol{\alpha}_i H.$$

Writing this differently, we arrive at the following:

Proposition 3.3. *The codimension of $T_{\boldsymbol{E}}$ is equal to the codimension of $T^r_{\boldsymbol{E}} := T_1(\ker T_2) \subseteq R$. This set can be written in the form*

$$T^r_{\boldsymbol{E}} = J + \{1, f_1, f_2\}\mathbb{R}[[H, H_2]], \tag{3.7}$$

where f_i are as defined above, and J is the ideal

$$J = \{\boldsymbol{\alpha}H | \boldsymbol{\alpha}H_2 = 0\}.$$

Generators of J From (3.4) it follows that the set of equivariant vector fields $\boldsymbol{\alpha}$ that leave H_2 fixed is generated, as an R-module, by

$$\begin{gathered}\mathbf{v}_3, \quad p\rho_2\mathbf{v}_1 - q\rho_1\mathbf{v}_2, \quad p\mathbf{v}_4 - q\mathbf{v}_6, \quad p\mathbf{v}_5 - q\mathbf{v}_7, \\ \psi\mathbf{v}_1 - \rho_1\mathbf{v}_4, \quad \chi\mathbf{v}_1 - \rho_1\mathbf{v}_5, \quad \psi\mathbf{v}_2 - \rho_2\mathbf{v}_6, \quad \chi\mathbf{v}_2 - \rho_2\mathbf{v}_7, \quad \chi\mathbf{v}_4 - \psi\mathbf{v}_6.\end{gathered}$$

The last five generators are actually multiples of $\mathbf{v}_3$, taking the relation into account. The first four, acting on H, yield the following generators of J:

$$\begin{aligned}h_0 &:= \psi^2 + \chi^2 - \rho_1^p\rho_2^q, \\ h_1 &:= \chi\frac{\partial H}{\partial \psi} - \psi\frac{\partial H}{\partial \chi}, \\ h_2 &:= 2\rho_1\rho_2\left(p\frac{\partial H}{\partial \rho_1} - q\frac{\partial H}{\partial \rho_2}\right) + \left(p^2\rho_2 - q^2\rho_1\right)\left(\chi\frac{\partial H}{\partial \chi} + \psi\frac{\partial H}{\partial \psi}\right), \\ h_3 &:= 2\psi\left(p\frac{\partial H}{\partial \rho_1} - q\frac{\partial H}{\partial \rho_2}\right) + \left(p^2\rho_1^{p-1}\rho_2^q - q^2\rho_1^p\rho_2^{q-1}\right)\frac{\partial H}{\partial \psi}, \\ h_4 &:= 2\chi\left(p\frac{\partial H}{\partial \rho_1} - q\frac{\partial H}{\partial \rho_2}\right) + \left(p^2\rho_1^{p-1}\rho_2^q - q^2\rho_1^p\rho_2^{q-1}\right)\frac{\partial H}{\partial \chi}.\end{aligned} \tag{3.8}$$

Note that we added the relation h_0, so that we can work in the free ring $R = \mathbb{R}[[\rho_1, \rho_2, \psi, \chi]]$.

Generators of J in the $1 : \pm 2$-resonance case Sect. 3.2.3 is valid for the $1 : \pm 2$ resonance case, up to the computation of generators of J. We give the details for that case here. Referring to (3.5), we find the following generators of the R-module of vector fields that leave H_2 invariant:

$$p\rho_2 V_1 - q\rho_1 V_2, \quad pV_4 - qV_6, \quad \psi V_1 - \rho_1 V_4$$

(where $p = 1, q = \pm 2$). The last generator is zero modulo the relation $\psi^2 - \rho_1^p\rho_2^q = 0$. The other two generators, acting on H, together with the relation, yield the following generators of J:

$$\begin{aligned}h_0 &:= \psi^2 - \rho_1^p\rho_2^q, \\ h_1 &:= 2\rho_1\rho_2\left(p\frac{\partial H}{\partial \rho_1} - q\frac{\partial H}{\partial \rho_2}\right) + (p^2\rho_2 - q^2\rho_1)\psi\frac{\partial H}{\partial \psi}, \\ h_2 &:= 2\psi\left(p\frac{\partial H}{\partial \rho_1} - q\frac{\partial H}{\partial \rho_2}\right) + (p^2\rho_1^{p-1}\rho_2^q - q^2\rho_1^p\rho_2^{q-1})\frac{\partial H}{\partial \psi}.\end{aligned} \tag{3.9}$$

3.2.4 Removing the χ-dependence

At this point we introduce a nondegeneracy condition, namely that $\frac{\partial H}{\partial \phi}$ and $\frac{\partial H}{\partial \psi}$ do not both vanish at the origin. (We would have needed this condition for other reasons later on anyway.) Under this condition it is possible to reduce the

dimension of the phase space by 1. This simplifies the computations. Again, see [Dui84].
Note that the module generated by V_4, $p\rho_2 V_2 - q\rho_1 V_3$, $pV_5 - qV_7$ and $pV_6 - qV_8$ is invariant under rotations in the ψ, χ-plane. This is obvious from the definition of the module, since H_2 is invariant under such rotations – indeed, H_2 is independent of ψ and χ.

By a rotation in the ψ, χ plane, we can arrange that $\frac{\partial H}{\partial \chi}(0) = 0$. Now assume that in this situation, $\frac{\partial H}{\partial \psi}(0) = d \neq 0$. By a further coordinate transformation, H can be made not to depend on χ at all, in the following way. Let

$$H = h_0 + \sum_{1<k<n} \tilde{f}_k(\psi) + \sum_{k \geq n} f_k(\psi, \chi),$$

where $n \geq 2$, $h_0 \in \mathbb{R}[[\rho_1, \rho_2, \psi]]$, $\tilde{f}_k$ is homogeneous of degree k in ψ, and f_k is homogeneous of total degree k in ψ and χ, both with coefficients in $\mathbb{R}[[\rho_1, \rho_2]]$. Write

$$f_n = \tilde{f}_n + \chi g_n,$$

with $\tilde{f}_n$ not depending on χ, and let $\boldsymbol{\alpha}$ be the vector field

$$\boldsymbol{\alpha} = -\frac{g_n}{d}\left(\chi \frac{\partial}{\partial \psi} - \psi \frac{\partial}{\partial \chi}\right).$$

It has time-1 flow

$$\boldsymbol{\alpha}^1(\psi, \chi) = \left(\psi - \frac{g_n}{d}\chi + O(|\psi, \chi|^{2n}), \chi + \frac{g_n}{d}\psi + O(|\psi, \chi|^{2n})\right).$$

Since $\frac{\partial h_0}{\partial \psi}(0) = d$ and $\frac{\partial h_0}{\partial \chi}(0) = 0$, we have $h_0 \circ \boldsymbol{\alpha}^1 = h_0 - \chi g_n + O(|\psi, \chi|^{n+1})$, and therefore

$$H \circ \boldsymbol{\alpha}^1 = h_0 + \sum_{1<k<n} \tilde{f}_k(\psi) + \tilde{f}_n(\psi) + \sum_{k \geq n+1} f_k(\psi, \chi).$$

Continuing in this way, all dependence in H of χ is removed, without changing the form of (3.8).

From now on we write R for the ring $\mathbb{R}[[\rho_1, \rho_2, \psi]]$, and we add the relation $\psi^2 - \rho_1^p \rho_2^q$ to the generators of the ideal J so that J is generated by

$$\begin{aligned}
h_0 &= \psi^2 - \rho_1^p \rho_2^q, \\
h_1 &= 2\rho_1\rho_2 \left(p\frac{\partial H}{\partial \rho_1} - q\frac{\partial H}{\partial \rho_2}\right) + \left(p^2\rho_2 - q^2\rho_1\right)\psi\frac{\partial H}{\partial \psi}, \\
h_2 &= 2\psi\left(p\frac{\partial H}{\partial \rho_1} - q\frac{\partial H}{\partial \rho_2}\right) + \left(p^2\rho_1^{p-1}\rho_2^q - q^2\rho_1^p\rho_2^{q-1}\right)\frac{\partial H}{\partial \psi}.
\end{aligned}$$

Note that these expressions are exactly equal to (3.9) of the $1 : \pm 2$-resonance case, where the removal of χ was done differently (namely, by a symplectic transformation).

3.3 Application to several resonances

In this section we compute standard bases for the left-right tangent space of Hamiltonians around several resonances. As a result, we get independent confirmation of the calculations in [Dui84], and explicit non-degeneracy conditions.

It is assumed that the Hamiltonian is in Birkhoff normal form, so that it can be written as a function of the fundamental circle invariants, which for the $p : q$ resonance are

$$\rho_1 = z_1\bar{z}_1, \quad \rho_2 = z_2\bar{z}_2, \quad \psi = \frac{1}{2}(z_1^p\bar{z}_2^{|q|} + \bar{z}_1^p z_2^{|q|}), \quad \chi = \frac{1}{2\mathrm{i}}(z_1^p\bar{z}_2^{|q|} - \bar{z}_1^p z_2^{|q|}).$$

We further assume that the dependence on χ is removed. Using the relation $\psi^2 - \rho_1^p\rho_2^q = 0$ the variable ψ can be made to appear to first order at most. The coefficients associated to the lowest-order terms are given names as follows:

(3.10)
$$\begin{aligned} H = {} & d_1\rho_1 + d_2\rho_2 + d_3\psi + d_4\rho_1^2 + d_5\rho_1\rho_2 + d_6\psi\rho_1 + d_7\rho_2^2 + d_8\psi\rho_2 + d_9\psi^2 + \\ & d_{10}\rho_1^3 + d_{11}\rho_1^2\rho_2 + d_{12}\psi\rho_1^2 + d_{13}\rho_1\rho_2^2 + d_{14}\psi\rho_1\rho_2 + d_{15}\psi^2\rho_1 + d_{16}\rho_2^3 + \\ & d_{17}\psi\rho_2^2 + d_{18}\psi^2\rho_2 + d_{19}\psi^3 + d_{20}\rho_1^4 + d_{21}\rho_1^3\rho_2 + d_{22}\psi\rho_1^3 + d_{23}\rho_1^2\rho_2^2 + \\ & d_{24}\psi\rho_1^2\rho_2 + d_{25}\rho_1 v 2^3 + d_{26}\psi\rho_1\rho_2^2 + d_{27}\rho_2^4 + d_{28}\psi\rho_2^3. \end{aligned}$$

The reduced tangent space is of the form

$$T^r_{\boldsymbol{E}} = \langle h_0, \ldots, h_k\rangle + \{f_0, \ldots, f_l\}\mathbb{R}[[g_1, \ldots, g_m]].$$

Once the basis $(\{h_i\}, \{f_i\}, \{f_i\})$ is extended to a standard basis, the codimension and deformation directions can be deduced from the leading monomials of the generators: The deformation directions are the monomials *not* in the basis, and the codimension is their number. The coefficients of the generator's leading monomials should be nonzero, as otherwise the codimension increases. This leads to the nondegeneracy conditions.

It often happens that a certain leading monomial can be reached through several reduction paths. The associated coefficient may be different for each path. Therefore we tried all different paths, to make sure no spurious nondegeneracy conditions were included.

Remark 3.4. *(Rigorous codimensions)* This is a computational study, and the codimensions obtained below are not rigorous, since we truncate at a certain degree. They are a rigorous *lower* bound, however. All this is rather academic, since the codimensions below are established, by different means, in [Dui84]. A related remark is that the set of nondegeneracy conditions obtained may not be complete. Since a full (non-truncated) standard basis will contain infinitely many elements, as is easily seen, there may in principle be infinitely many (polynomial) nondegeneracy conditions. Indeed, in some cases we find more of such conditions than appear in [Dui84].

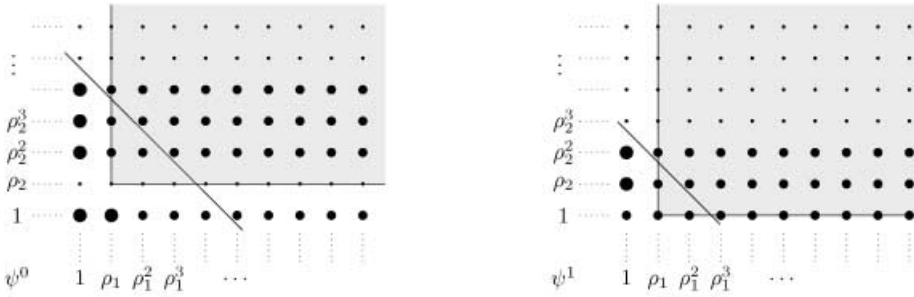

Fig. 3.1 Standard basis of LR-tangent space for the 1 : 2 resonance.

3.3.1 The 1:2 resonance

We use the expressions (3.9) for the generators of J, truncated at order 9 in the z_i variables. We use a grading of the monomials with $\deg(\rho_1) = \deg(\rho_2) = 2$, $\deg(\psi) = 3$, and the ordering satisfies $\psi^2 < \rho_1^3 < \rho_2^3$. The computation of the standard basis then yields the following leading monomials:

$$\begin{aligned}
\mathsf{LM}(\{h_i\}) &= \{\psi\rho_1, \rho_1\rho_2, \psi^2\},\\
\mathsf{LM}(\{g_i\}) &= \{\rho_1, \psi\},\\
\mathsf{LM}(\{f_i\}) &= \{1, \rho_1, \rho_2^2, \rho_2^3, \rho_2^4, \psi\rho_2, \psi\rho_2^2\}.
\end{aligned}$$

This standard basis is depicted graphically in Fig. 3.1. Monomials are represented by lattice points in $\mathbb{N}^3$. Since one of the ideal generators has leading monomial ψ^2, the interesting things happen in the ψ^0 and ψ^1 slices. The monomials in the ideal are those in the grey rectangles. Fat dots denote f_i-generators, and the medium-sized dots correspond to monomials obtained by multiplying an f_i and an element of the algebra. The diagonal line, finally, shows where we truncated. From the figure, it is seen that the codimension is 1, and that the deformation term that makes the Energy–Momentum map versal, is ρ_2. This is called the *detuning* term.

The requirement that, for each basis element, the coefficients of the leading monomials do not vanish, leads to the following nondegeneracy conditions:

$$\begin{aligned}
d_3 &\neq 0,\\
8d_3^2 - 2d_4 + d_5 + 4d_7 &\neq 0.
\end{aligned} \tag{3.11}$$

A *normal form* for the Hamiltonian behind this tangent space is a simple function (a polynomial, for example) with few parameters, but which nevertheless captures all bifurcations. A sufficient condition for this is to include all terms whose parameters appear in the nondegeneracy conditions; perturbations in the other terms will not change the type of the singularity. This condition is generally not necessary. However, for our purposes it is useful to be able to choose

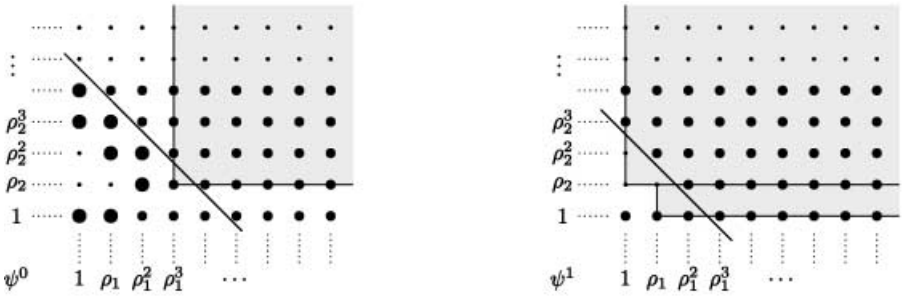

Fig. 3.2 Standard basis of LR-tangent space for the 1 : 3 resonance.

parameters such that the normalizing transformation is the identity in leading order. It turns out that e.g.

$$H = \frac{1}{2}\rho_1 + \left(\frac{1}{4} + \mu_1\right)\rho_2 + d_3\psi + d_5\rho_1\rho_2 \tag{3.12}$$

is a suitable normal form. Here d_3 and d_5 are (fixed) parameters, and μ_1 is the *detuning parameter*.

3.3.2 The 1:3 resonance

For this resonance, the reduced tangent space was calculated up to order 8 in the z_i variables. The variable ψ has degree 4, so that it appears at most to second degree. We use a monomial ordering satisfying $\psi < \rho_2^2 < \rho_1^2$. With this ordering the leading monomials of the standard basis are

$$\begin{aligned}
\mathsf{LM}(\{h_i\}) &= \{\psi\rho_1, \psi^2, \psi\rho_2, \rho_1^3\rho_2\},\\
\mathsf{LM}(\{g_i\}) &= \{\rho_1, \psi\},\\
\mathsf{LM}(\{f_i\}) &= \{1, \rho_1, \rho_1^2\rho_2, \rho_1^2\rho_2^2, \rho_1\rho_2^3, \rho_1\rho_2^2, \rho_2^4, \rho_2^3\}.
\end{aligned}$$

A graphical representation of this standard basis is given in figure 3.2. Now the codimension is 3, with corresponding deformation directions ρ_2, $\rho_1\rho_2$ and ρ_2^2. The nondegeneracy conditions for this resonance are somewhat complicated, so we introduce the following abbreviations:

$$\begin{array}{lll}
a = \frac{1}{2}(d_{10} + d_{11}) & c = d_4 - d_5 - 3d_7 & e = \frac{1}{2}(d_6 + d_8)\\
b = \frac{1}{2}(d_{10} - d_{11}) & d = 2d_4 - 3d_5 & f = -2d_6 - 3d_8
\end{array}$$

In terms of these quantities, the nondegeneracy conditions are the following:

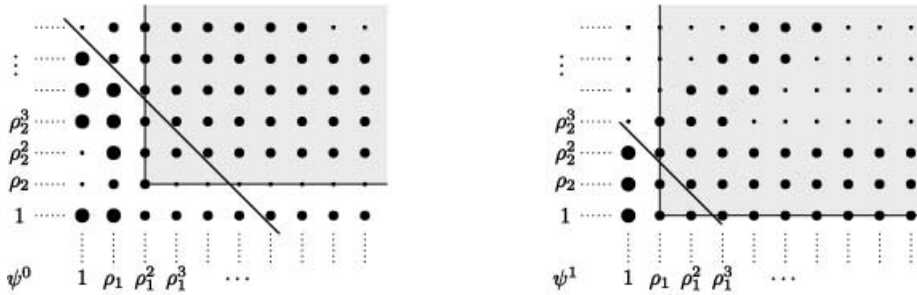

Fig. 3.3 Standard basis of LR-tangent space for the 1 : 4 resonance.

$d_3 \neq 0$,
$d_4 + 3d_5 - 27d_7 \neq 0$,
$c \neq 0$,
$d \neq 0$,
$3^6(9c+2d)d_3^4 + 216d(12c^2+3cd+2d^2)d_3^2 + 16d^2(9c^3-6c^2d-3cd^2+2d^3) \neq 0$,
$216bd_3^3 - 54ded_3^2 + 4(6bc^2+acd-19bcd+8bd^2-3cdd_{13})d_3 +$
$8(d-c)d(6ce-de+cf) \neq 0$,
$5832bd_3^5 - 1458ded_3^4 + 27(168bc^2+10acd-228bcd+64bd^2-21cdd_{13})d_3^3$
$-108d(12c^2e-25cde+4d^2e-c^2f-2cdf)d_3^2$
$+4(216bc^4+36ac^3d-612bc^3d-38ac^2d^2+580bc^2d^2+10acd^3-228bcd^3+$
$+32bd^4-108c^3dd_{13}+99c^2d^2d_{13}-21cd^3d_{13})d_3$
$-16(3c-2d)(2c-d)(3c-d)d(6ce-de+cf) \neq 0$.

A normal form for this singularity is for example

$$H = \frac{1}{2}\rho_1 + \left(\frac{1}{6}+\mu_1\right)\rho_2 + d_3\psi + d_4\rho_1^2 + (d_5+\mu_2)\rho_1\rho_2 + (d_7+\mu_3)\rho_2^2 + d_{10}\rho_1^3 + d_{13}\rho_1\rho_2^2.$$

3.3.3 The 1:4 resonance

For this resonance we again chose the obvious grading, $\deg(\rho_1) = \deg(\rho_2) = 2$ and $\deg(\psi) = 5$, and the monomial order defined by $\psi^2 < \rho_2^5 < \rho_2^5$. The truncation degree was set at 11, resulting in the following standard basis:

$$\begin{aligned}
\mathsf{LM}(\{h_i\}) &= \{\rho_1^2\rho_2, \psi\rho_1, \psi^2\},\\
\mathsf{LM}(\{g_i\}) &= \{\rho_1, \rho_1\rho_2\},\\
\mathsf{LM}(\{f_i\}) &= \{1, \rho_1, \rho_1\rho_2^2, \rho_1\rho_2^3, \rho_1\rho_2^4, \rho_2^5\rho_2^4, \psi\rho_2^2, \psi\rho_2, \rho_2^3, \psi\}.
\end{aligned}$$

The codimension is 2, with deformation terms ρ_2 and ρ_2^2. The nondegeneracy conditions are the following:

$$
\begin{aligned}
&d_3 \neq 0, .\\
&d_4 - 2d_5 \neq 0,\\
&3d_4 - 8d_5 - 16d_7 \neq 0,\\
&d_4 - 16d_7 \neq 0,\\
&d_5 - 8d_7 \neq 0,\\
&d_4 - 4d_5 + 16d_7 \neq 0,\\
&5d_4^2 + 32d_5^2 - 128d_5d_7 + 256d_7^2 + 32d_4d_7 - 24d_4d_5 \neq 0.
\end{aligned}
$$

A normal form is for example

$$H = \frac{1}{2}\rho_1 + \left(\frac{1}{8} + \mu_1\right)\rho_2 + d_3\psi + d_4\rho_1^2 + d_5\rho_1\rho_2 + (d_7 + \mu_2)\rho_2^2.$$

3.4 Spring-pendulum in 1:2 resonance

In this section we shall analyze the spring-pendulum system in the 1 : 2 resonance, by exhibiting a polynomial model of the Energy–Momentum map, and computing the reparametrizations that connect the model to the original system. The bifurcation analysis of the model leads to a bifurcation diagram, together with a 'catalog' of possible dynamics as depicted in phase diagrams. Using the explicit reparametrization the bifurcation curves are pulled back to the space of the spring pendulum's original parameters, giving full information as to which subset of the full set of possible dynamics actually occurs, and where bifurcations take place in terms of the original parameters.

This section's analogue for the planar reduction case is section 2.3, but this section is organized slightly differently. We start with a bifurcation analysis of the polynomial normal form, and we give pictures of the bifurcation and phase space diagrams. This is followed by the computation of the explicit reparametrizations, of which we only give the results. These are then used to pull back the bifurcation curves to the original parameter space.

3.4.1 Bifurcation analysis of the 1:2-resonant normal form

In Sect. 2.3 we encountered a third-order polynomial normal form, with a rather simple bifurcation structure. The normal form for this case is less simple, involving degree-four terms, which complicates the computations. The normal form for the 1 : 2-resonant system is:

$$\boldsymbol{E}^{\mu} = (H^{\mu}, H_2) = (H_2 + \mu\rho_2 + a\psi + b\rho_1\rho_2, H_2)\,, \tag{3.13}$$

see Sect. 3.3.1. Here we wrote H_2 for the quadratic part $\frac{1}{2}\rho_1 + \frac{1}{4}\rho_2$ as usual; a and b are fixed coefficients, and μ is the deformation parameter; see (3.10), (3.12). In Hamiltonian polar coordinates $z_i = r_i e^{2\pi i\phi_1}$, the fundamental invariants become $\rho_i = r_i^2$ and $\psi = r_1 r_2^2 \cos(\phi_1 - 2\phi_2)$. These variables are used in the sequel.

We restrict to the flow-invariant level sets $2H_2 = \lambda$, for small λ, which corresponds to small-energy deviations from the elliptic equilibrium. The function H^μ restricted to such level sets has critical points precisely where $\boldsymbol{E}^\mu$ has critical points, namely where $\mathrm{grad}(H_2)$ is parallel to $\mathrm{grad}(H^\mu)$. A short calculation shows that a necessary condition[1] for this is $\sin(\phi_1 - 2\phi_2) = 0$. It is now convenient to introduce $\epsilon := \cos(\phi_1 - 2\phi_2)$, so that $\epsilon = \pm 1$. Now $\mathrm{grad}(H_2)$ and $\mathrm{grad}(H^\mu)$ are vectors in $\mathbb{R}^2 \ni (r_1, r_2)$, and such vectors are parallel if their outer product vanishes. The resulting curve of critical points is

$$r_2 \left(-2\mu r_1 - 2a\epsilon r_1^2 - 2b r_1^3 + \left(\tfrac{1}{2}a\epsilon + b r_1\right) r_2^2\right) = 0. \tag{3.14}$$

This implies that $r_2 = 0$ is always a critical point; it corresponds to the 'short periodic orbit' that always exists.

Equation (3.14), with the solution $r_2 = 0$ divided out, can be solved for r_2^2. Obviously, critical points (dis)appear when the solution r_2^2 of (3.14) passes through 0. This leads to a bifurcation curve in the μ, λ-plane implicitly given by

$$(\mu + 2b\lambda)^2 - 2a^2\lambda = 0. \qquad \textit{(pitchfork bifurcation)} \tag{3.15}$$

The parabolic equation (3.15) has solutions for nonnegative λ only. Since the critical points emanate from $r_2 = 0$ which itself is a critical point throughout the bifurcation, this is a pitchfork bifurcation. The bifurcation occurs at the point

$$(r_1, r_2, \psi, \chi) = \left(\left|\frac{1}{a}\mu + \frac{b}{a^3}\mu^2 + \frac{2b^2}{a^5}\mu^3\right|, 0, 0, 0\right) + O(\mu^4). \tag{3.16}$$

Other bifurcations occur when the curve of critical points (3.14) in the r_1, r_2-plane become tangent to level curves of H_2. When this happens, a small change in the level λ will (generically) create or destroy two critical points. One of these will be a saddle, the other a center or a *node*, so that this is a saddle–node bifurcation. The tangency condition is that $\mathrm{grad}(H_2)$ and the gradient of the left-hand-side of (3.14) be parallel, and using the outer product once more we get the bifurcation equation

$$r_2 \left(2\mu + 6a\epsilon r_1 + 10 b r_1^2 - b r_2^2\right) = 0. \tag{3.17}$$

Bifurcations occur at simultaneous solutions, in r_1, r_2, μ, λ, of $2H_2 = \lambda$, (3.14) and (3.17). This solution curve can be found by computing a Gröbner basis with respect to an elimination term order (see Sect. 6.2.1) of the ideal generated by these three polynomials. Since only three generators are involved, we can get the same result (with, essentially, the same computation) using resultants.[2] Computing the resultant of the pair $2H_2 - \lambda$, (3.14) and of (3.14), (3.17) with respect

[1] We exclude the degenerate case $r_1 = r_2 = 0$.

[2] The resultant of two polynomials, with respect to the variable x, is their GCD with respect to the divisibility condition $x^a | x^b \Leftrightarrow a \leq b$, i.e., it vanishes iff the polynomials have a common root in x.

to r_2, eliminates this variable, and reduces the system of 3 polynomial equations to a system involving only 2. The resultant with respect to r_1 subsequently reduces this system to the following cubic curve in the μ, λ-plane, along which the saddle–node bifurcations occur:

(3.18)
$$\begin{aligned} &27a^4\lambda + 9a^2b^2\lambda^2 + 32b^4\lambda^3 - 126a^2b\lambda\mu \\ &-96b^3\lambda^2\mu + 9a^2\mu^2 + 96b^2\lambda\mu^2 - 32b\mu^3 = 0, \end{aligned} \qquad \textit{(saddle–node bifurcation)}$$

where we used that $\epsilon^2 = 1$, and we first divided out two factors r_2 corresponding to the pitchfork bifurcation. Note that the cubic curve is independent of ϵ now. Also note that the curve has quadratic contact with the line $\lambda = 0$ in $\mu = 0$. By expanding around 0 it turns out that the curve has no solutions $\lambda > 0$ around $(\lambda, \mu) = (0, 0)$, for all values of the coefficients a, b (provided $b \neq 0$). It has a critical point at $(\mu, \lambda) = (\frac{5a^2}{16b}, \frac{-a^2}{16b^2})$.

Not all points on the cubic correspond to saddle–node bifurcations. The reason is that due to the constraint $2H_2 = \lambda = \rho_1 + \frac{1}{2}\rho_2 = r_1^2 + \frac{1}{2}r_2^2$, the solutions for the r_i may be imaginary. The 'turning points' on the cubic, where real solutions turn into imaginary ones, is where either r_1^2 or r_2^2 pass through 0. From (3.14) it follows that $r_1 \neq 0$ at critical points (provided $\lambda \neq 0$). So we turn our attention to the equation $r_2 = 0$. The curve of pitchfork bifurcations (3.15) is just the curve where critical points satisfy $r_2 = 0$, hence the turning points are intersections of the cubic (3.18) with the parabola (3.15).

To compute these intersection points we compute the resultant of the two curves. With respect to λ this is

$$4096b^{10}\mu^2(-a^2 + 4b\mu)^2(153a^4 - 352a^2b\mu + 256b^2\mu^2).$$

From this we conclude that (3.18) and (3.15) have quadratic contact at $(\mu, \lambda) = (0, 0)$ and $(\mu, \lambda) = (\frac{a^2}{4b}, \frac{a^2}{4b^2})$. The last factor is quadratic in μ, with discriminant $-32768a^4b^2$. Provided that neither a nor b vanishes, this does not contribute additional (real) zeros.

Since the part of the cubic connecting the turning points $(\mu, \lambda) = (0, 0)$ and $(\frac{a^2}{4b}, \frac{a^2}{4b^2})$ passes through the $\lambda < 0$ region, namely through the critical point $(\frac{5a^2}{16b}, \frac{-a^2}{16b^2})$, we conclude that saddle–node bifurcations occur only for

$$\lambda > \frac{a^2}{4b^2}. \qquad \textit{(condition for saddle–node bifurcation)}$$

In order to get a useful expression for μ in terms of λ, we expand the cubic (3.18) around the turning point. Writing $\Lambda = \lambda - \frac{a^2}{4b^2}$ we get

$$\mu = \frac{a^2}{4b} + \frac{b^3}{3a^2}\Lambda^2 - \frac{10b^5}{27a^4}\Lambda^3 + \frac{47b^7}{81a^6}\Lambda^4 + O(\Lambda^5). \qquad \textit{(saddle–node bifurcation)}$$

We also computed the bifurcation locus, around the turning point. Writing $\mathrm{M} := \mu - \frac{a^2}{4b}$, then saddle–node bifurcations occur for $\mathrm{M}/b \geq 0$ at points which have the following expansion in $\sqrt{\mathrm{M}}$:

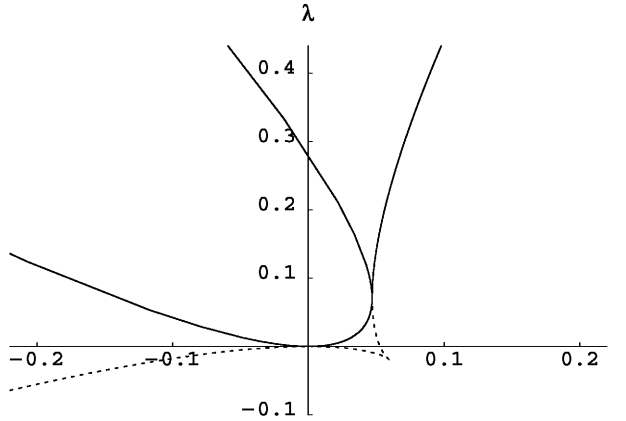

Fig. 3.4 Bifurcation curves of the normal form (3.13), for $a = \frac{1}{4}$ and $b = \frac{1}{3}$. The parabola is a curve of pitchfork bifurcations; along the singular cubic curve saddle–node bifurcations occur. Dashed segments correspond to non-physical states of the system (λ out of bounds, leading to imaginary values of state variables).

(3.19)

$$
\begin{aligned}
(r_1, r_2^2, \psi, \chi) = \Bigg(& \operatorname{sign}(b) \left(\tfrac{|a|}{2b} + \sqrt{\tfrac{\mathrm{M}}{3b}} + \tfrac{4\mathrm{M}}{9|a|} + \tfrac{40\sqrt{b\mathrm{M}^3}}{27\sqrt{3}a^2} + \tfrac{512b\mathrm{M}^2}{243|a^3|} \right), \\
& 4|a| \sqrt{\tfrac{\mathrm{M}}{3b^3}} + \tfrac{32\mathrm{M}}{9b} - \tfrac{80}{27|a|} \sqrt{\tfrac{\mathrm{M}^3}{b}} + \tfrac{832\mathrm{M}^2}{243a^2}, \\
& - \operatorname{sign}(a) \left(2a^2 \sqrt{\tfrac{\mathrm{M}}{3b^5}} + \tfrac{28|a|\mathrm{M}}{9b^2} + \tfrac{8(6\sqrt{3}-5)}{27} \sqrt{\tfrac{\mathrm{M}^3}{b^3}} + \tfrac{80(16-3\sqrt{3})\mathrm{M}^2}{243|a|b} \right), \\
& 0 \quad \Bigg) \quad + O(|\mathrm{M}|^{5/2}).
\end{aligned}
$$

3.4.2 Pictures

The surface on which H^μ lives is the level set $2H_2 = \lambda$, which is a 3-torus in $\mathbb{R}^4$. Using the $\mathbb{S}^1$-symmetry to divide out one dimension, we can make 2-dimensional pictures of level sets of H^μ on this surface. There are two natural ways of choosing coordinates, which are both singular but have their singularities in different locations on the 3-torus. We give pictures for both sets of coordinates.

The bifurcation diagram consists of the parabola (3.15) of pitchfork bifurcations, and the cubic (3.18) of saddle–node bifurcations. For $a = 1/4$ and $b = 1/3$ these curves are shown in Fig. 3.4. Note that around the origin, the bifurcation diagram is similar to Fig. 2.5.

In Fig. 3.5 the level curves of H^μ are plotted, for fixed $2H_2 = \lambda$ with $\lambda > \frac{a^2}{4b^2}$, so that a saddle–node bifurcation is expected. The two sets of pictures correspond to the Poincaré sections $\phi_2 = 0$ and $\phi_1 = 0$, corresponding to the pendulum and

the spring having zero velocity, respectively. The fundamental invariants ρ_1, ρ_2, ψ in Cartesian coordinates on either Poincaré section are

	$\rho_1:$	$\rho_2:$	$\psi:$
$\phi_2 = 0:$	$x^2 + y^2$	$4\lambda - 2(x^2 + y^2)$	$2x(2\lambda - x^2 - y^2)$
$\phi_1 = 0:$	$2\lambda - \frac{1}{2}(x^2 + y^2)$	$x^2 + y^2$	$(x^2 - y^2)\sqrt{2\lambda - (x^2 + y^2)/2}$

Note that the short periodic orbit $\rho_2 = 0$ corresponds to the origin in the section $\phi_1 = 0$ (the right-hand column of pictures), whereas it corresponds to the outer circle $x^2 + y^2 = 2\lambda$ in the section $\phi_2 = 0$. Similarly, the origin in the left-hand column, i.e., $\rho_2 = 0$, corresponds to the outer circle $x^2 + y^2 = 4\lambda$ of the other.

Besides the saddle–node and pitchfork bifurcations found in section 3.4.1, a fourth 'bifurcation' is observed. It is caused by the coincidence of the level through $\rho_1 = 0$ and the critical value of the saddle emanating from the saddle–node bifurcation. Since the subset $\rho_1 = 0$ (spring not oscillating) is not an invariant subset, this coincidence appears to be a bifurcation only because of the choice of coordinates in the right-hand column, where $\rho_1 = 0$ corresponds to the outer circle. This should be contrasted to the situation in the left-hand column, where the outer circle corresponds to $\rho_2 = 0$ (pendulum not oscillating), which *is* an invariant subset.

3.4.3 Inducing the system from the model

The Hamiltonian equation for the spring-pendulum system is derived in section 2.3.1. For reference we quote equation (2.7) up to order 4:

$$H^0(x,y) := \frac{x_1^2 + y_1^2}{2} + a_1\frac{x_2^2 + y_2^2}{2} - 4a_2x_2y_1y_2 - 8a_3x_2^4 + 8a_4x_2^2y_1^2 + 8a_5x_2^2y_2^2 + O(|x_i, y_i|^5).$$

After Birkhoff normalization around 1 : 2 resonance, the Hamiltonian can be written in terms of the fundamental invariants ρ_1, ρ_2, ψ as in equation (3.10), analogous to H^n in Sect. 2.3.2. The leading part, up to fourth order in phase variables, of equation (3.10), is

$$H^n = d_1\rho_1 + d_2\rho_2 + d_3\psi + d_4\rho_1^2 + d_5\rho_1\rho_2 + d_7\rho_2^2 + O(|x_i, y_i|^5), \tag{3.20}$$

with coefficients depending on those of the original Hamiltonian as

$$\begin{aligned} &d_1 = \frac{1}{2}, \quad d_2 = \frac{a_1}{2}, \quad d_3 = -2a_2, \quad d_4 = 0, \\ &d_5 = \frac{4(-2a_2^2 + a_4 + 2a_1a_4)}{1 + 2a_1}, \quad d_7 = \frac{-2(a_2^2 + (1 + 2a_1)(3a_3 - a_5))}{1 + 2a_1}. \end{aligned} \tag{3.21}$$

Generally, the Birkhoff normalized system depends on χ. However, since our system has a time-reversibility symmetry under which χ is sent to $-\chi$, the

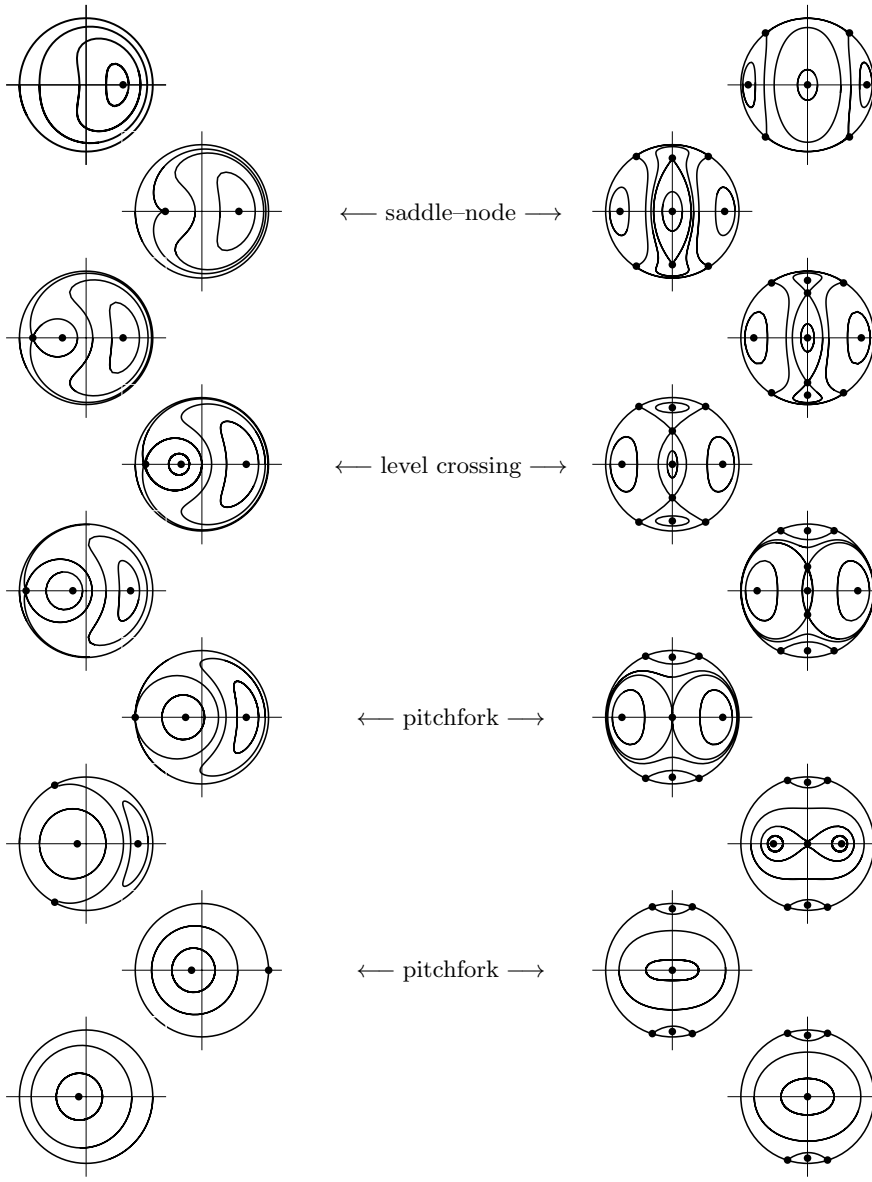

Fig. 3.5 Bifurcations of the Energy–Momentum map normal form around the 1:2 resonance (large λ). The left-hand column corresponds to the section $\phi_2 = 0$ with a return time $\approx 4\pi$; the section $\phi_1 = 0$ (right-hand column) has a return time $\approx 2\pi$.

normalized Hamiltonian only depends on even powers of χ. By using the relation $\psi^2+\chi^2 = \rho_1\rho_2^2$, all of these terms can be removed. Hence, a second normalization to remove terms involving χ is not necessary.

In the new variables, the conserved quantity is $\lambda := \rho_1 + \frac{1}{2}\rho_2$. Pulling this back to old coordinates yields

$$\lambda = \left(x_1^2 + y_1^2\right) + \frac{1}{2}\left(x_2^2 + y_2^2\right) + \frac{8a_2}{1+2a_1}\left(-x_1x_2^2 + 2x_2y_1y_2 + x_1y_2^2\right) + O(|x_i, y_i|^4).$$

(For λ up to fourth order terms, see (2.8).)

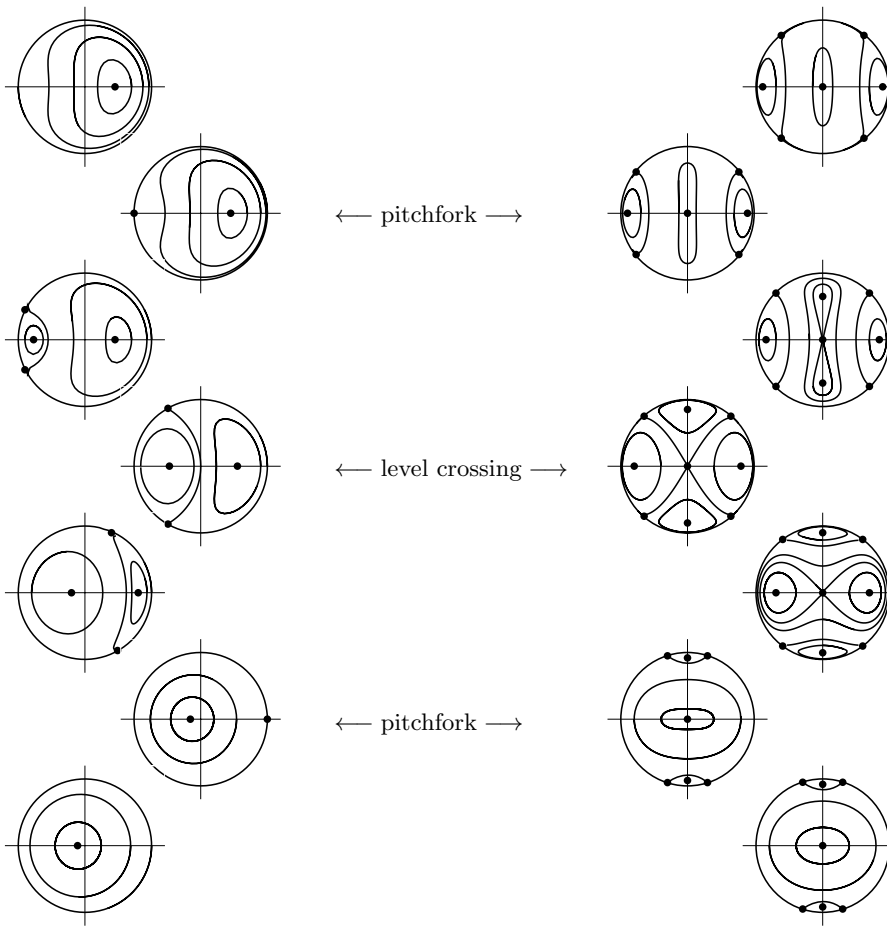

Fig. 3.6 Bifurcations of the Energy–Momentum map normal form around the 1:2 resonance (small λ).

Birkhoff nondegeneracy conditions Depending on the order to which Birkhoff normalization is performed, a number of nondegeneracy conditions are encountered. From the expressions for d_5 and d_7 the condition $a_1 \neq -1/2$ follows

immediately. If normalization is continued up to eighth order, we should exclude the following values for a_1:

$$a_1 \neq -\frac{3}{2},\ a_1 \neq -1,\ a_1 \neq -\frac{1}{2},\ a_1 \neq -\frac{1}{4},\ a_1 \neq 0,\ a_1 \neq \frac{1}{4},\ a_1 \neq 1,\ a_1 \neq \frac{3}{2}.$$

(We remark that as the normalization order is increased, more and more rational values of a_1 must be excluded. In the limit of infinite order, all rational numbers[3], except the value $\frac{1}{2}$ around which we normalize, should be excluded. This is related to the non-convergence of the normalizing formal power series. Effectively, this means that the higher the order to which normalization is performed, the smaller is the allowed deviation of a_1 from the resonant value.)

Energy–momentum map nondegeneracy conditions In Sect. 3.3.1 the tangent space to an arbitrary Hamiltonian (3.20) is computed, assuming that it is Birkhoff normalized around the 1 : 2 resonance. This tangent space has minimal codimension (namely 1) if two nondegeneracy conditions are met. We may pull back these to the space of original parameters, simply by substituting the expressions for the coefficients d_i. This yields the following nondegeneracy conditions:

$$\begin{aligned} &0 \neq a_2, \\ &0 \neq 4(1+4a_1)a_2^2 - (1+2a_1)(6a_3 - a_4 - 2a_5). \end{aligned}$$

Normalizing transformation From now on we suppose that the nondegeneracy conditions hold. We may then compute a standard basis for the left-right tangent space of H^n. This serves as input for Kas and Schlessinger's algorithm, with which we can compute transformations that connect H^n to the versal unfolding H^u obtained in Sect. 3.3.1, namely

$$H^u_\mu = \frac{1}{2}\rho_1 + \left(\frac{1}{4} + \mu\right)\rho_2 + a\psi + b\rho_1\rho_2. \tag{3.22}$$

This model has the drawback that generically a Hamiltonian H^n cannot be induced from it by transformations that are the identity to first order. Theoretically this is no problem. An practical nuisance however is that for such models, Kas and Schlessinger's algorithm does not yield a finite part of the formal power series in a finite number of steps.

It turns out that adding a second deformation direction, for instance $c\rho_1^2$, solves this problem. For reasons of convenience, and while it does not complicate the analysis, we chose to add *two* extra deformation directions, and use the model

$$H^U_\mu = \frac{1}{2}\rho_1 + \left(\frac{1}{4} + \mu\right)\rho_2 + a\psi + b\rho_1^2 + c\rho_1\rho_2 + d\rho_2^2. \tag{3.23}$$

[3] modulo a scaling by a factor 2

By following the calculation of Sect. 3.4.1 we then arrive at this equation for the pitchfork bifurcation:

$$(\mu + (b-c)\lambda)^2 - a^2\lambda = 0,$$

which occurs at

$$(r_1, r_2, \psi, \chi) = \left(\left|\frac{1}{a}\mu + \frac{b-c}{a^3}\mu^2 + \frac{2(b-c)^2}{a^5}\mu^3\right|, 0, 0, 0\right) + O(\mu^4).$$

Now we discuss the computation of the inducing transformation. Since the unfolding H^U has fewer terms than the target Hamiltonian H^n, it is more efficient to compute the inverse transformation, going from H^U to H^n. In particular, the expressions for the standard basis of H^U's tangent space are much cleaner than H^n's.

Let $\mathbb{R}^d \ni (a_1, a_2, \ldots)$ be the space of parameters of the Birkhoff-normalized system H^n. We computed functions

$$\begin{aligned} h(a_i) &: \mathbb{R}^p \to \mathbb{R}, \\ A(\rho_1, \rho_2, \psi; a_i) &: \mathbb{R}^3 \oplus \mathbb{R}^d \to \mathbb{R}^3, \\ B(y_1, y_2; a_i) &: \mathbb{R}^2 \oplus \mathbb{R}^d \to \mathbb{R}^2 \end{aligned}$$

such that these induce the actual system H^n from the versal unfolding H^U_μ:

$$H^n \quad = \quad B \circ (H^U_{h(\mu)}, H_2) \circ A.$$

These transformations depend on the parameters a, b, c, d of the versal model (3.22). Several choices of these parameters yield transformations that are the identity to first order, which is related to there being one deformation direction too much for this purpose. The natural choice is of course

$$a = d_3 = -2a_2, \qquad b = d_4 = 0, \qquad c = d_5, \qquad d = d_7,$$

see also (3.21). With this choice, the resulting transformations are

$$\begin{aligned} h = \quad & -\frac{1}{4}(1 - 2a_1) \\ A_1(\rho_1, \rho_2, \psi) = \quad & \rho_1 + \left(\frac{16a_2^2}{(1+2a_1)^2} - \frac{8(4a_3 + a_4 + 4a_4)}{3(1+2a_1)} - \frac{4a_6}{3a_2}\right)\rho_1\rho_2 + \\ & \left(\frac{-192a_2^3}{(1+2a_1)^2} + \frac{32a_2(8a_3 + 5a_4 + 8a_5)}{3(1+2a_1)} + \frac{32a_6}{3}\right)\psi\rho_1 + h.o.t. \\ A_2(\rho_1, \rho_2, \psi) = \quad & \rho_2 + \left(\frac{-32a_2^2}{(1+2a_1)^2} + \frac{16(4a_3 + a_4 + 4a_4)}{3(1+2a_1)} + \frac{8a_6}{3a_2}\right)\rho_1\rho_2 + \\ & \left(\frac{-192a_2^3}{(1+2a_1)^2} + \frac{32a_2(8a_3 + 5a_4 + 8a_5)}{3(1+2a_1)} + \frac{32a_6}{3}\right)\psi\rho_1 + h.o.t. \\ A_3(\rho_1, \rho_2, \psi) = \quad & \psi + \left(\frac{-288a_2^3}{(1+2a_1)^2} + \frac{16a_2(8a_3 + 5a_4 + 8a_5)}{(1+2a_1)} + 16a_6\right)\psi^2 + \\ & \left(\frac{-8a_2^2}{(1+2a_1)^2} + \frac{4(4a_3 + a_4 + 4a_4)}{3(1+2a_1)} + \frac{2a_6}{3a_2}\right)(4\psi\rho_1 - \psi\rho_2) + h.o.t. \end{aligned}$$

$$
\begin{aligned}
B_1(y_1, y_2) = \quad & y_1 + O(|y_1, y_2|^3 + |a_i|^3) \\
B_2(y_1, y_2) = \quad & y_2 + \left(\frac{-24a_2^2}{(1+2a_1)^2} + \frac{4(8a_3 + 5a_4 + 8a_5)}{3(1+2a_1)} + \frac{4a_6}{3a_2} \right) (4y_1y_2 - y_2^2) + \\
& + O(|y_1, y_2|^3 + |a_i|^3)
\end{aligned}
$$

Here *h.o.t.* denote terms of order n or higher in the phase variables, and order 3 or higher in the parameters a_i.

It remains to find the bifurcation curves, in terms of the detuning parameter $1-2a_1$ and the integral λ. Because the transformations above are not symplectic, the λ-level sets of H^U transformed by this coordinate transformation are not dynamically invariant, and do not correspond to λ-level sets of H^n. Hence, to find the bifurcation curves, we need to find the location of bifurcations in H^U, transform it back to original variables via A^{-1}, and compute λ at those phase points. Since A is the identity to first order, its inverse is easy to find. The pitchfork bifurcation in H^U occurs on the line $\rho_2 = \psi = 0$, and since A does not involve ρ_1^2 (in fact, it does not include ρ_1^3 terms either) the inverse also does not contain these terms. Hence, on line $\rho_2 = \psi = 0$ the map A^{-1} is the identity to at least third order.

Calculating λ at the point (3.4.3) and expanding in $1 - 2a_1$ results in the following expression for the pitchfork bifurcation:

(3.24)
$$
\lambda = \frac{(1-2a_1)^2}{64a_2^2} + \frac{(a_2^2 - a_4)(1-2a_1)^3}{128a_2^4} + \frac{(a_2^4 - 10a_2^2a_4 + 5a_4^2)(1-2a_1)^4}{1024a_2^6} + h.o.t.,
$$

where the *h.o.t.* stand for $O((1-2a_1)^5)$ terms. It agrees with (2.14) found using the planar reduction method.

For the saddle–node bifurcation it is not possible to find a similar equation. The reason is that this bifurcation occurs at a finite distance from the origin, and only for $O(1)$ values of the detuning parameter $1 - 2a_1$, see (3.19), and the transformation A and its inverse are only valid near the origin.

Table 3.1 Comparison of bifurcation values, found numerically and analytically. Error bounds in last digit(s) of measured quantities are given

H	a_1	a_2	a_3	a_4	a_5	$\lambda_{\text{measured}}$	$\lambda_{\text{predicted}}$
.004	$.47513 \pm 1$	.1	0	$-.3$	.2	$.008025 \pm 5$	$--$
.004	$.48405 \pm 5$	.1	0	$-.3$	.2	$.008000 \pm 2$	$.00286 \pm 2$
.004	$.5562 \quad \pm 2$	.1	0	$-.3$	.2	$.007999 \pm 1$	$.060 \pm 1$
.004	$.46454 \pm 1$	.1	0	$-.01$	.35	$.008000 \pm 4$	$--$
.004	$.46550 \pm 1$	.1	0	$-.01$	.35	$.008000 \pm 3$	$.007988 \pm 5$
.004	$.53705 \pm 1$	.1	0	$-.01$	.35	$.007999 \pm 1$	$.007991 \pm 4$
.0004	$.48882 \pm 1$	.1	0	$-.01$	.05	$.00080000 \pm 1$	$.0007991 \pm 14$
.0004	$.51144 \pm 1$	.1	0	$-.01$	.05	$.00080000 \pm 1$	$.0007997 \pm 13$

Numerical Poincaré sections To validate (3.24) we numerically computed an iso-energy Poincaré map, using the section $y_2 = 0$ and increasing; i.e., transversal to the long periodic orbit. We fixed the energy, and coefficients $a_2, a_3, \ldots$, while varying a_1 to find the bifurcation value. The value of λ was then measured along trajectories close to the bifurcation point.

Error bounds in a_1 correspond to values that bracket the actual bifurcation value. These bracketing values were determined by computing phase diagrams and inspecting them visually. The error in $\lambda_{\text{predicted}}$ was obtained by propagating the errors in a_1. Error bounds in $\lambda_{\text{measured}}$ correspond to the observed variation in the computed value for λ along a trajectory. This error bound may be too low, as it obviously depends on the trajectory. An alternative estimation method, estimating the remainder in the series (2.8) for λ, seems difficult.

Another perturbing effect, which influences the error bound in $\lambda_{\text{measured}}$, is the effect of *chaotic* dynamics, that is, the effect of the higher-order perturbation terms that are thrown away in order to arrive at an integrable model. For the energies considered, this effect is extremely small. However, this is a statement of belief rather than a hard fact. It is support by the fact that the nonintegrable effects are due to a flat perturbation, and that the chaotic regime begins to have a 'noticeable' effect only for energies a factor 10 to 100 higher than we consider.

The agreement of the predicted bifurcation value of λ and its actual value is excellent for small values of a_4 and small values of the energy. For the case $a_4 = -0.3$, the three consecutive terms in (3.24) are of similar magnitude, which suggests that more terms are needed for convergence, in agreement with the large deviation of $\lambda_{\text{predicted}}$ from the observed value of λ.

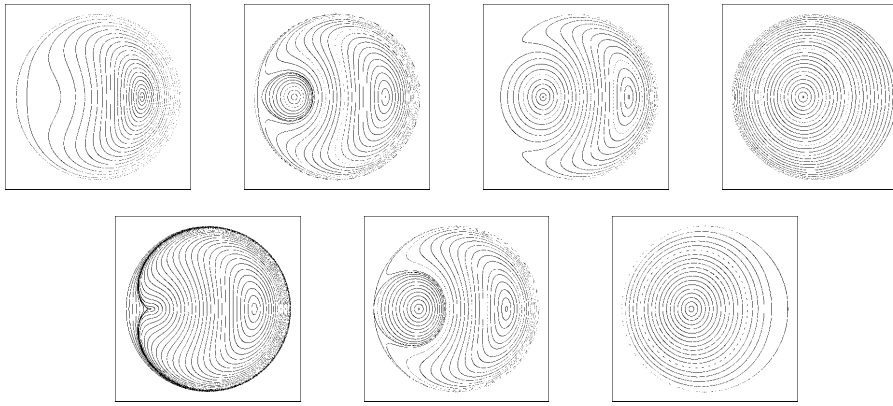

Fig. 3.7 Bifurcations in the Poincaré section around the 1:2 resonance, for $H = 0.004$, $a_2 = 0.1$, $a_3 = 0$, $a_4 = -0.3$, $a_5 = 0.2$, other coefficients 0, and a_1 increasing from left to right: 0.47,0.47513, 0.48, 0.48405, 0.49, 0.5562, 0.57.

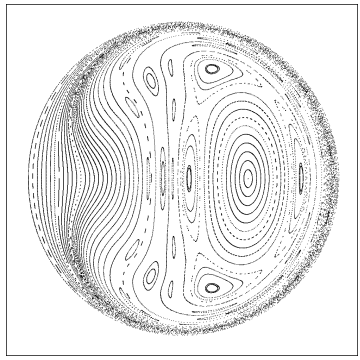

$a_1 = 0.46$

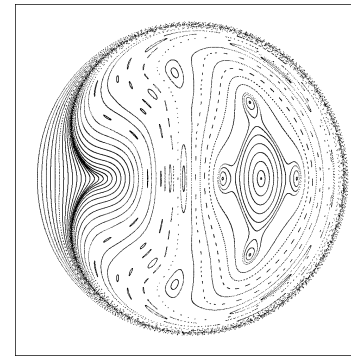

$a_1 = 0.47$

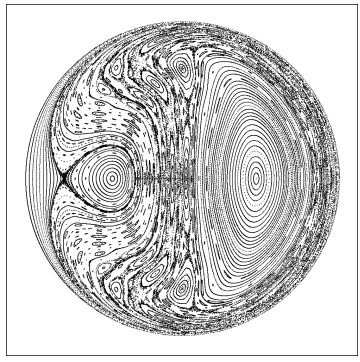

$a_1 = 0.48$

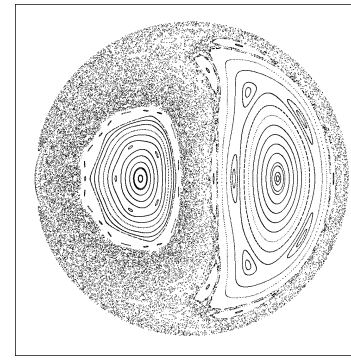

$a_1 = 0.51$

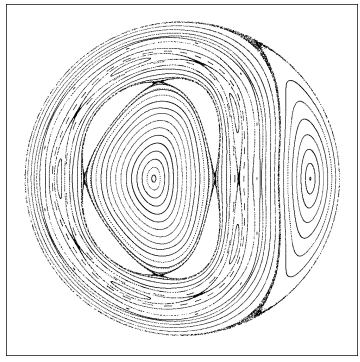

$a_1 = 0.60$

Fig. 3.8 Some large-energy Poincaré sections: $H = 0.1$. Chaotic regimes and subharmonic bifurcations are clearly visible, with the backbone of Fig. 3.7 still present.